Climate Dynamics (2006) 26: 677–685
DOI 10.1007/s00382-005-0108-2

Matthew D. Therrell · David W. Stahle
Lydia P. Ries · Herman H. Shugart

Tree-ring reconstructed rainfall variability in Zimbabwe

Received: 10 August 2005 / Accepted: 5 December 2005 / Published online: 10 January 2006

Abstract We present the first tree-ring reconstruction of rainfall in tropical Africa using a 200-year regional chronology based on samples of *Pterocarpus angolensis* from Zimbabwe. The regional chronology is significantly correlated with summer rainfall (November–February) from 1901 to 1948, and the derived reconstruction explains 46% of the instrumental rainfall variance during this period. The reconstruction is well correlated with indices of the El Niño-southern oscillation (ENSO), and national maize yields. An aridity trend in instrumental rainfall beginning in about 1960 is partially reproduced in the reconstruction, and similar trends are evident in the nineteenth century. A decadal-scale drought reconstructed from 1882 to 1896 matches the most severe sustained drought during the instrumental period (1989–1995), and is confirmed in part by documentary evidence. An even more severe drought is indicated from 1859 to 1868 in both the tree-ring and documentary data, but its true magnitude is uncertain. A 6-year wet period at the turn of the nineteenth century (1897–1902) exceeds any wet episode during the instrumental era. The reconstruction exhibits spectral power at ENSO, decadal and multi-decadal frequencies. Composite analysis of global sea surface temperature during unusually wet and dry years also suggests a linkage between reconstructed rainfall and ENSO.

M. D. Therrell (✉) · L. P. Ries · H. H. Shugart
Department of Environmental Sciences, University of Virginia, Charlottesville, VA, 22904 USA
E-mail: therrell@virginia.edu
Tel.: +1-434-9243186

D. W. Stahle
Department of Geosciences, University of Arkansas, Fayetteville, AR, 72701 USA

1 Introduction

Southern Africa experiences a high degree of rainfall variability, both in space and time. Because much of this region is arid to semiarid, rainfall represents a vital resource for its people and environment. For example, in Zimbabwe a large majority of the population is directly dependent on maize agriculture, about half of which is grown on less productive communal lands (Makarau and Jury 1996; Phillips et al. 1998). In recent decades severe droughts have caused drastic reductions in maize production in southern Africa (e.g., Cane et al. 1994). A number of studies have analyzed rainfall fluctuations over southern Africa in the modern period and have identified several patterns of variability and associated forcing mechanisms. For example, drought in southern Africa has been linked to variability in the El Niño-southern oscillation (ENSO) system as well as sea surface temperatures (SSTs) in portions of the Atlantic and Indian Oceans adjacent to southern Africa (Tyson 1986; Nicholson and Entekhabi 1986; Ropelewski and Halpert 1987, 1989; Mason and Jury 1997; Nicholson and Kim 1997).

The instrumental record of climate is relatively short in much of southern Africa, but much can be learned from long proxy climate time series. Physical proxies of past climate such as speleothems and lake sediment records are available for a few sites in southern Africa (e.g., Holmgren 2002; Verschuren et al. 2000), and historical records such as missionary correspondence and lake level records have also been used to study past climate in the region (Nicholson 1979, 1981; Vogel 1989; Lindesay and Vogel 1990; Nash and Endfield 2002). Dunwiddie and LaMarche (1980) developed one of the first tree-ring chronologies in southern Africa, using *Widdringtonia cedarbergensis*, and other research has been focused on *Podocarpus* species (Thackeray 1996). Unfortunately, neither of these species has so far proven very useful for climate reconstruction (e.g., February and Stock 1998; February and Gagen 2003). Stahle (1999) reported the development of short tree-ring chronologies in Kenya, and Stahle et al. (1999) developed climate sensitive tree-ring chronologies in Zimbabwe using *Canthium burtii* and *P. angolensis*. Subsequent tree-ring research on *Pterocarpus* and other species in Namibia and Zambia also appears promising (Trouet et al. 2001; Fichtler et al. 2004; Trouet 2004).

Known locally as Mukwa, (*P. angolensis* D.C.) is a deciduous tropical hardwood reaching about 15 m in height. It is a member of the *Fabaceae* family. The genus *Pterocarpus* Jacq. is found throughout the tropics with the exception of Australia and Madagascar (von Breitenbach 1973). Mukwa is widely distributed across southern Africa growing from sea level in Mozambique to over 1,600 m in Tanzania (Fig. 1). The climatic range of Mukwa is restricted to the 'Dry Subhumid Region', which has a single rainy season, mean annual rainfall of 500–1,250 mm, and mean minimum temperatures of 20°C in the warmest month and 4°C in the coldest month. (von Breitenbach 1973). Mukwa prefers well drained soils, has "excessive" light demands, and is highly adapted to fire (von Breitenbach 1973). In addition, like the closely related Indo–Malayan 'Padouk' (e.g., *P. dalbergioides* and *P. macrocarpus*), Mukwa is an economically important timber species.

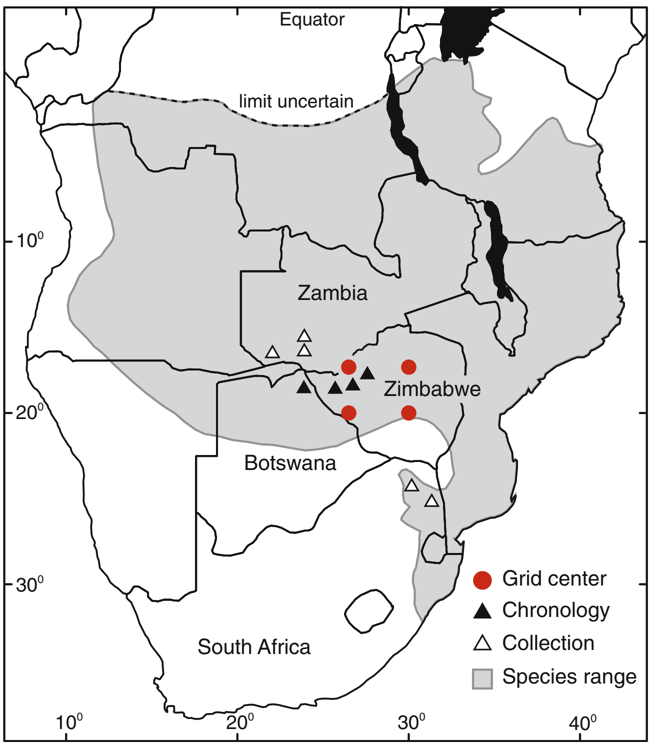

Fig. 1 The natural range of *Pterocarpus angolensis* (*gray shading*; von Breitenbach 1973; Coates Palgrave 1983) extends across much of tropical southern Africa. We have developed tree-ring chronologies at four sites in Botswana and Zimbabwe (*black triangles*) and have collected samples from five additional sites in Zambia and South Africa (*white triangles*). The center points of the four 2.5×3.5° CRU precipitation data grid boxes used in this study are also shown (*red circles*)

Stahle et al. (1999) demonstrated that Mukwa trees growing in western Zimbabwe produce definitive annual rings and that ring width growth is significantly correlated with monthly and seasonal precipitation totals from December through February (DJF) over a large area of central southern Africa (i.e., 'Region 60' for 1900–1996; Nicholson 1994). Fichtler et al. (2004) also found that Mukwa ring width growth at two sites in northern Namibia is significantly correlated with regional rainfall and other climate factors in that area. Shackleton (2002) found that Mukwa growth in the South African lowveld was strongly related to rainfall over a 6-year period.

In this paper, we present a regional reconstruction of annual rainfall for the past 201 years using tree-ring chronologies of Mukwa from Zimbabwe, and 2.5×3.75° gridded precipitation data. We discuss tree-ring reconstructed estimates of rainfall variability during severe drought episodes, and examine the relationship between tree-ring reconstructed rainfall and potential forcing mechanisms such as ENSO and anomalous SSTs in the southern Atlantic and Indian Oceans. We also discuss the relationship between the rainfall reconstruction and maize yield in Zimbabwe, as well as new tree ring collections from Botswana, South Africa, and Zambia and the potential for developing additional tree-ring sites in southern Africa.

2 Data and methods

Tree-ring samples from two previously reported collections of Mukwa from Sikumi and Mzola forests in western Zimbabwe (Stahle et al. 1999), as well as samples from logs cut for lumber in the Matabeleland province of western Zimbabwe. and from the Pandamatanga region of Botswana were used in the current study (Fig. 1). In addition to the tree-ring chronologies that we have developed for this study we have also collected Mukwa samples in South Africa and recently in Zambia (Fig. 1). Samples from the Matabeleland and Pandamatanga sites were used to develop two new individual chronologies and we have also developed a regional chronology using the combined raw ring width data (21 trees, 36 series) from the three Zimbabwe sites (Sikumi, Matabeleland, Mzola), which we use for the reconstruction of regional precipitation (Fig. 2).

Development of the Matabeleland and Pandamatanga chronologies was difficult because few samples were available, and many of these were difficult to crossdate. Although Mukwa generally crossdates quite well (Stahle et al. 1999), the complex anatomy of this semi-ring porous species requires that cross-sections rather than conventional increment cores be used for analysis. Even when using cross sections, long periods of suppressed growth were often difficult to date. Our experience indicates that samples with a cross sectional surface of at least 10 cm in width from a large number of different age class trees are required for chronology

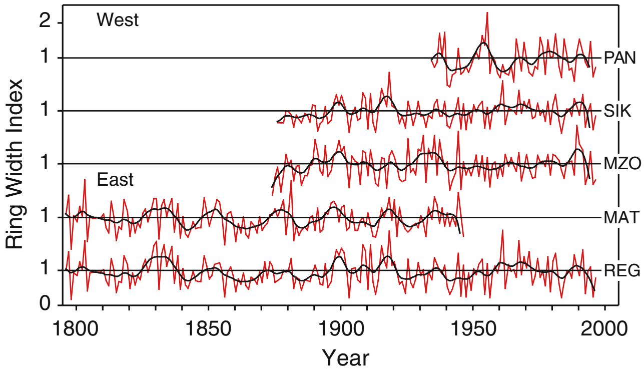

Fig. 2 The annual values (*red*) and 10-year smoothing spline values (*black*) for tree-ring chronologies of *P. angolensis* from northeastern Botswana (Pandamatanga) and western Zimbabwe (Sikumi, Mzola, and Matabeleland, respectively), and a regional chronology using the three chronologies from Zimbabwe. Each chronology is significantly correlated with all others, and most display coherent decadal variability despite being widely separated. The Pandamatanga chronology is well correlated with the chronologies from Zimbabwe, but was not included in the regional chronology because no series from this site currently overlap the calibration period used for the precipitation reconstruction. (Fig. 3)

development. For further discussion of Mukwa dating see Stahle et al. 1999.

All samples were analyzed using the same standard dendrochronological techniques including the skeleton plot methods of cross-dating (Douglass 1941; Stokes and Smiley 1996), measurement on a stage micrometer to a precision of 0.001 mm, and quality control of cross-dating with the computer program COFECHA, which checks dating accuracy using correlation analyses (Holmes 1983). There is fairly strong inter-series correlation among the 36 series used for the regional chronology ($r = 0.63$). The raw ring width measurements were conservatively detrended to remove long-term ring width decline associated with non-climatic growth trends. Each series was detrended only once using a negative exponential curve ($n = 6$) or linear regression curve of any slope ($n = 30$). Chronology indices were calculated as the ratio of tree growth to curve value. The resulting indices were then averaged together into an index chronology using a robust mean value function, which minimizes the impact of outliers on the computation of the mean index values. The detrending and chronology computation processes were carried out using the program ARSTAN (Cook 1985; E. Cook personal communication). The signal strength of the regional chronology is fairly stable through time based on running series of average correlations (RBAR, i.e., the mean correlation coefficient among tree-ring series; Briffa 1995) and the expressed population signal (EPS statistic; Cook and Kairiukstis 1990). The regional chronology RBAR is 0.59, and ranges from 0.32 around 1900 to 0.81 around 1875. The EPS statistic is considered acceptable at levels above 0.85 (Cook and Kairiukstis 1990) and the regional Mukwa chronology meets or exceeds that level from about 1820 onward.

Data from four 2.5×3.75° grid squares from the CRU global gridded precipitation dataset (constructed and supplied by CRU, University of East Anglia, Norwich, UK; Hulme 1992, 1994; Hulme et al. 1998; version 1.0) were used to develop a regional monthly rainfall series. The CRU data extend from 1900 to 1998 and were extracted from the National Climatic Data Center's Global Historical Climatology Network (GHCN). Although no topographical weighting was performed during the grid interpolation, this is unlikely to have much influence given the minimal topographical relief over most of the study area.

We also use 5×5° gridded monthly instrumental SST anomaly data available globally from 1856 to 1991 produced by Kaplan et al. (1998). These data are primarily based on merchant ship samples that have been interpolated using an optimal smoothing scheme to fill data voids. Anomalies are based on the 1951–1980 mean value at each grid point (Kaplan et al. 1998).

Seasonal (November through February) precipitation totals for each of the four grids were compiled and these totals were then averaged into a regional precipitation series. This precipitation series was then used as the basis for a regression analysis to develop estimates of precipitation based on ring width. Mukwa ring width in our study area probably begins sometime in November and definitely ends after January. Most of the seasonal rainfall and crop growth in the region also occurs after 1 January (Fig. 3a), so we identify annual tree growth by the year growth ends. We do not employ the so called 'Schulman shift', which assigns the annual value to the calendar year in which growth begins and has been used

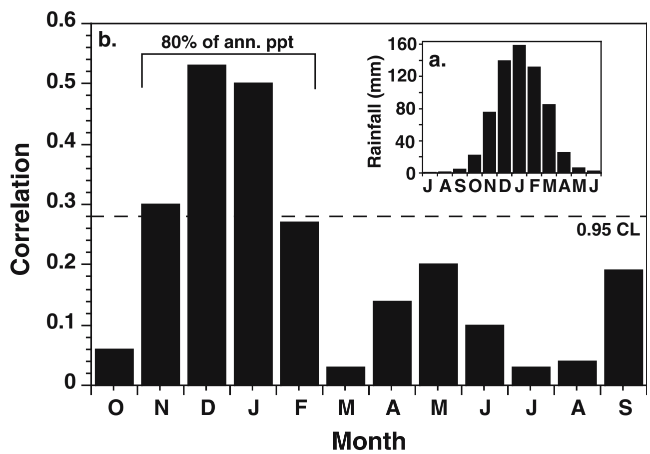

Fig. 3 a Monthly rainfall totals from July through June. **b** Correlation coefficients (with 95% confidence level) computed between the regional tree-ring chronology and monthly rainfall totals in Zimbabwe (based on the regional average of four CRU grid points). The chronology is significantly correlated with wet-season total rainfall ($r = 0.69$, $p \leq 0.0001$). Experimental correlation analyses between the regional tree-ring chronology and station level temperature data from the GHCN network indicate that mean monthly temperature probably has little effect on ring width, though prior November mean temperatures are weakly negatively correlated with ring width ($r = -0.27$, $p \leq 0.05$)

in dendrochronological studies elsewhere in the southern hemisphere (Schulman 1956).

A variety of statistical tests were performed on the estimates provided by the model. These included the Pearson correlation coefficient and the Pearson correlation coefficient after first-differencing the series, which tests the relationship between the observed and reconstructed time series after removal of low-frequency variance (Fritts 1990). Possible autocorrelation in the residuals from the regression model was examined using the Durbin-Watson statistic (Draper and Smith 1981). The reduction of error (RE) test (Fritts 1990) examines the fraction of observed precipitation variance estimated by the tree-ring data in both the calibration and verification periods. We also used spectral analysis (Jenkins and Watts 1968) to evaluate the frequency domain properties of the reconstruction.

3 Results

The regional tree-ring chronology is correlated with monthly rainfall totals for Zimbabwe during the summer rainy season from prior November through February (Fig. 3b). Rainfall in these four months represents over 80% of the annual (July–June) total in Zimbabwe. Autoregressive modeling did not identify significant persistence in either the tree-ring or precipitation data, and a bivariate regression model was used in order to calibrate the tree-ring chronology with the seasonalized precipitation data. We used a split-period calibration and verification procedure to develop and test the regression model. The independent data (precipitation) were evenly split into early (1901–1948) and late periods (1949–1996) and a calibration model was constructed for the early half and then verified against the withheld data during the later period. We chose to develop the reconstruction calibration on the early period based on the stronger regression statistics in this period.

Linear regression was used to calibrate the regional tree-ring chronology with summer precipitation from 1901 to 1948. The calibration equation for the model period (1901–1948) is

$$\hat{Y}_t = 311.70 + 205.275X_t \tag{1}$$

where $\hat{Y}t$ is the estimated summer precipitation value and X_t is the corresponding tree-ring index value (t = year in both cases). The tree-ring data explain 46% of the summer rainfall variance (r^2 adjusted for loss of 1° of freedom; Draper and Smith 1981), and there is no significant trend in the regression residuals (Durbin Watson test, not significant; Durbin and Watson 1950).

The reconstruction passes most of the verification tests. The correlation between observed and reconstructed rainfall from 1949 to 1996 is $r = 0.43$ ($p \leq 0.01$), which is a significant drop from the calibration period (Fig. 4). However, the first-differenced correlation from 1949 to 1996 is $r = 0.57$ ($p \leq 0.0001$), indicating that low-frequency variability (probably decadal) is not coherent between the reconstructed and observed rainfall data. The sign test is not significant, indicating poor agreement (29 hits, 19 misses) between the observed and reconstructed rainfall series from 1949 to 1996. The cross-products means test (Fritts 1990) also fails significance testing. However, the more stringent RE statistic during the verification period is RE = 0.19 indicating reasonable skill in the reconstruction, though the coefficient of efficiency test is only slightly lower (0.18).

The relatively low correlation and verification statistics calculated between the observed and reconstructed rainfall during the verification period is difficult to explain, because the period includes the latter half of the twentieth century when the quality of the rainfall data should be better. The replication of the chronology declines somewhat during this period (Fig. 5). There may also be instability in the tree-growth sensitivity to rainfall, or the instrumental regional rainfall average may itself include important spatial or temporal variability over time. For example, there appears to be a slight shift in rainfall toward the early part of the rainy season in the verification period when mean October rainfall increases 34%, November and December means rise slightly (~3%), and January and February rainfall decreases (~5%). But this hardly seems sufficient to account for the drastic change in correlation coefficients between the two periods. We are unaware of any important changes in the quality of station data that contribute to the gridded data and the four grids do not show any appreciable change in their relationship over time, but relevant changes in the climate data cannot be ruled out.

One shortcoming of the reconstruction that does not appear to be confined to the verification period is the reconstruction's tendency to underestimate moisture extremes (Fig. 4). This is a common issue with dendroclimatic reconstructions (Fritts 1976). Typically drought years are better estimated than extremely wet conditions because moisture deficit is normally the most important limiting factor to tree growth. In the Zimbabwe rainfall reconstruction almost all extreme wet and dry years (> 1 std) are underestimated. However reconstructed rainfall values in extreme drought years are generally more closely estimated than wet years (Fig. 4). The only real way to improve the reconstruction will be to add additional tree-ring sites and species to the tree-ring chronology network.

4 Analysis of the reconstruction

Using the calibration model (Eq. 1) we reconstructed rainfall over Zimbabwe from 1796 to 1996 (Fig. 5). Outstanding features of the reconstruction include seven consecutive years of drought from 1882 to 1888 (mean = 452 mm vs. the 201 year reconstruction mean of 509 mm). In the instrumental period, this episode is surpassed only by the eight-year drought from 1989 to

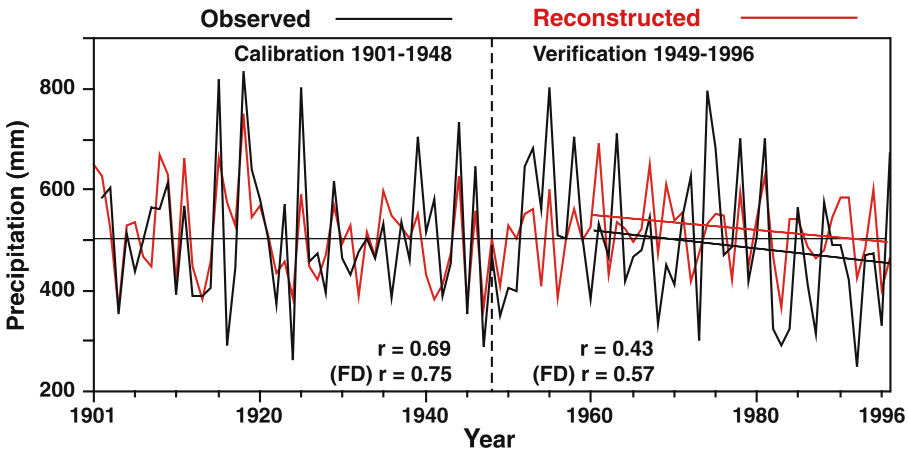

Fig. 4 Observed (*black*) and tree-ring reconstructed (*red*) summer rainfall totals in Zimbabwe from 1901 to 1996 (the mean of 502 mm is based on instrumental data from 1901 to 1996). The simple and first differenced correlation coefficients are indicated for the calibration and verification sub-periods. Note the aridity trend in the observed and reconstructed rainfall data after ~1960 (*black and red regression lines*, respectively)

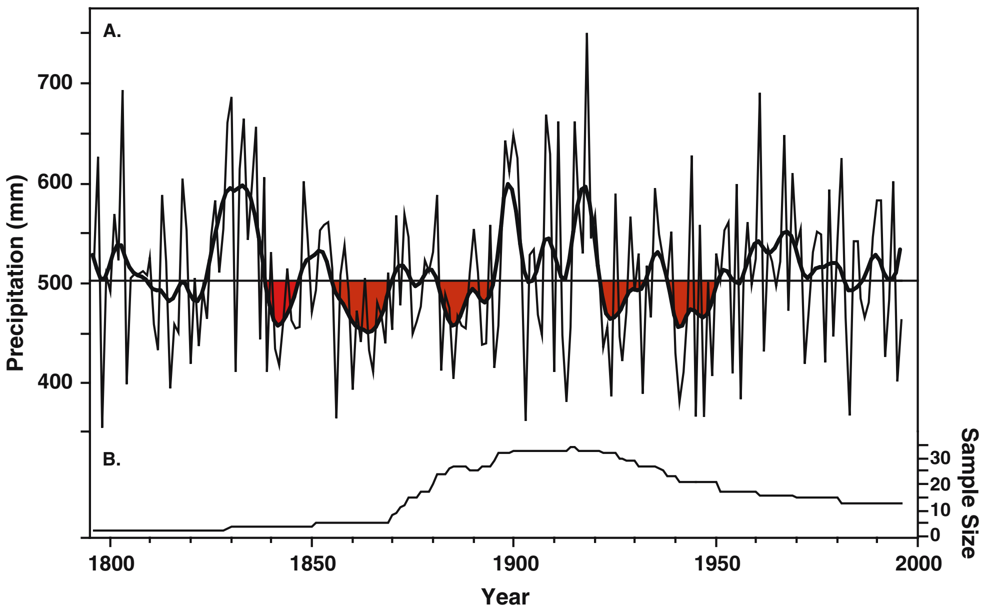

Fig. 5 **a** Annual (*thin line*) and 10-year smoothing spline (*heavy line*) values of reconstructed November–February regional rainfall from 1796 to 1996. Prominent decadal and multi-decadal variability is evident in the smoothed times series, which is supported by the spectral analysis of the reconstruction (Fig. 7). Several severe and prolonged drought periods in the reconstruction are highlighted (*red shading*). **b** Sample depth (series) over time (total sample depth = 21 trees, 36 series)

1995 (mean = 418 mm vs. the 96 year observational mean of 502 mm; Fig. 4). The decadally smoothed series indicates that the late nineteenth century drought lasted from 1882 to 1896, which approximately equals the drought of the 1940s shown in both the observational (Fig. 4) and reconstructed data (Fig. 5). The 1880s–1890s drought was followed by six unbroken years of high rainfall from 1897 to 1902. This wet period was unequalled by any similar event in the instrumental period, though similar episodes occurred in the 1910s and 1950s (Figs. 4, 5).

A decadal-scale drought in the mid nineteenth century (1859–1868) appears to have persisted longer than any decadal drought in the observational record. Other interesting events shown in the reconstruction include droughts in the 1820s and 1840s as well a wet period in the 1830s (Fig. 5). However, as Fig. 5b indicates, replication is quite low prior to 1870, so the reconstruction should only be considered preliminary and will require additional sample replication to confirm.

Contemporary historical sources in the Kalahari region (Botswana) report drought conditions in these areas that were often coincident with episodes shown in the reconstruction. For example, the drought shown in the reconstruction between 1882 and 1888 may be related to drought conditions in Botswana that apparently began in some areas in 1877 and became 'widespread' between 1884 and 1886 (Nash and Endfield 2002), but the reconstruction does not confirm the 'widespread' drought conditions reported in Botswana from 1894 to 1899. There is evidence for reconstructed drought in 1892–1893 and 1895–1896, but 1897–1899 are among the wettest 3 years in the reconstruction.

The mid-nineteenth century drought shown in the reconstruction (Fig. 5) may be related to 'widespread' drought reported in Botswana from 1857 to 1865 (Nash and Endfield 2002). The year 1860, which is the lowest reconstructed value during this period was described in a contemporary account from Botswana, as a season of 'severe and universal drought' with 'food of every description' being 'exceedingly scarce' and the losses of cattle being 'very severe' (Nash and Endfield 2002).

The reconstruction also provides evidence for both positive and negative multi-decadal rainfall trends of similar magnitude to the one beginning in the latter half of the twentieth century (Figs. 4, 5). These trends may be real features of long-term rainfall in Zimbabwe but will need confirmation with additional tree-ring data.

Spectral analysis (Jenkins and Watts 1968) of the reconstructed precipitation time series indicates that the tree-ring estimates of Zimbabwe summer rainfall have significant ($p \leq 0.05$) concentrations of variance at periods near 3.4, 9, and 20 years (Fig. 6). The weak 20-year peak in variance accounts for 4.3% of the overall variance, and may be associated with multi-decadal scale variability in the range of 16–20 years, which has been observed in southern Africa rainfall series and other records (Tyson et al. 2002). We also observe a broad spectral peak between 8 and 10 years that accounts for 8.2% of the relative variance and is significant at the 99% level at 8.89 years.

Two spectral peaks between 3.33 and 3.48 years accounts for 9.0% of the variance and may be related to ENSO variability, which has been shown by several studies to influence precipitation in southern Africa (Tyson 1986; Ropelewski and Halpert 1987; Mason and Jury 1997; Nicholson and Kim 1997). In fact, the rainfall reconstruction is weakly correlated with the CRU seasonal (DJF) southern oscillation index (SOI; $r = 0.21$; $p = 0.011$) over the entire overlap period from 1866 to 1996. Several studies have indicated that the influence of ENSO on precipitation in known teleconnection regions is variable on decadal scales (e.g., Allan et al. 1996; Krishna Kumar et al. 1999; Torrence and Webster 1999) and similar variability in ENSO influence has been noted in southern Africa (e.g., Moron and Ward 1998). The simple correlation between the rainfall reconstruction and DJF SOI is quite variable with correlations in non-overlapping 20 year blocks ranging from $r = 0.49$ (1926–1945) to $r = 0.00$ (1946–1965). The ENSO influence on rainfall in Zimbabwe is greater at the beginning (October) and end of the wet season (March; Mason 2001),

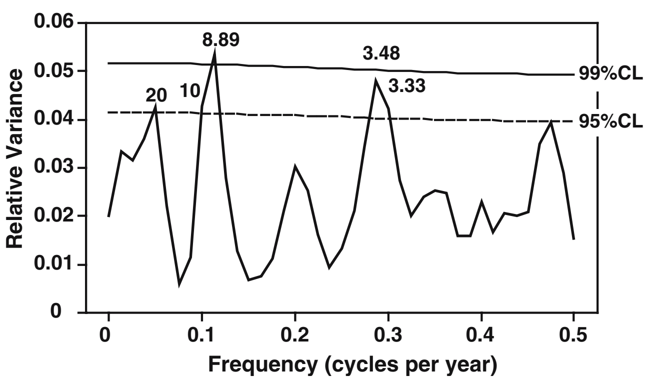

Fig. 6 Spectral analysis of the rainfall reconstruction indicates that significant spectral power is concentrated at periods of 20, 8–10 and ~3.4 years. The 3.4-year peak may reflect the influence of ENSO

when rainfall is not well correlated with the growth of Mukwa in the region (Fig. 3).

Composite analyses of seasonal (DJF) SSTs during the ten driest and ten wettest years in the rainfall reconstruction since 1857 also indicate an ENSO influence in Zimbabwe (Fig.7). In Fig. 7a, warm anomalies are evident in the eastern equatorial Pacific corresponding to El Niño conditions. Analysis of CRU seasonal (DJF) southern oscillation index (SOI) values, indicates that all but one (1956) of these ten dry years were below average (more negative). Moderate warm anomalies are also evident off southwestern Africa and in the central Indian Ocean. Warm (cool) SSTs in the southern Atlantic and Indian Oceans have been linked to dry (wet) conditions in southern Africa particularly during El Niño events (Nicholson and Entekhabi 1987; Jury 1996; Nicholson and Kim 1997; Mason 2001).

The global SST pattern for the ten wettest years in the reconstruction (Fig. 7b) indicates weak cool conditions in the eastern equatorial Pacific (La Niña-like), as well as cool SSTs in the southern Atlantic. These features are both consistent with wetness in southern Africa (Nicholson and Entekhabi 1987; Jury 1996). Other features include a large cool anomaly in the northwestern Pacific, which is probably not related to rainfall in Zimbabwe.

The tree-ring reconstruction is weakly correlated with national maize yields in Zimbabwe (FAO 2004) from 1970 to 1996 ($r = 0.43$; $p \leq 0.25$). However, this correlation increases to $r = 0.64$ ($p \leq 0.006$) during the period 1980–1996 after Zimbabwe achieved independence and promoted increased smallholder maize farming and planting of hybrid varieties, which resulted in substantial increases in the amount of rain fed rather than irrigated maize. These results are preliminary of course, and need to be confirmed with additional tree-ring and maize yield data. Nevertheless they suggest that an expanded network of *P. angolensis* chronologies may provide valuable insight into the history of maize production and perhaps other crops in southern Africa. Cane et al. (1994) found that the NINO3 index explains 61% of the variability in maize yield in Zimbabwe between 1970 and 1993. This relationship may offer some potential for prediction of maize yields. However, the tree-ring data indicate that the ENSO influence on tree growth in Zimbabwe is non-stationary. The opportunity for skillful prediction of precipitation, tree growth, and maize yield in Zimbabwe based on ENSO may rise and fall on a multi-decadal time scale. Identifying the cause of this multi-decadal non-stationarity could have enormous socioeconomic importance.

5 Conclusions

This study provides the first high-resolution tree-ring reconstruction of rainfall for Zimbabwe. The reconstruction is well correlated with instrumental precipitation data from the twentieth century, and gives estimates

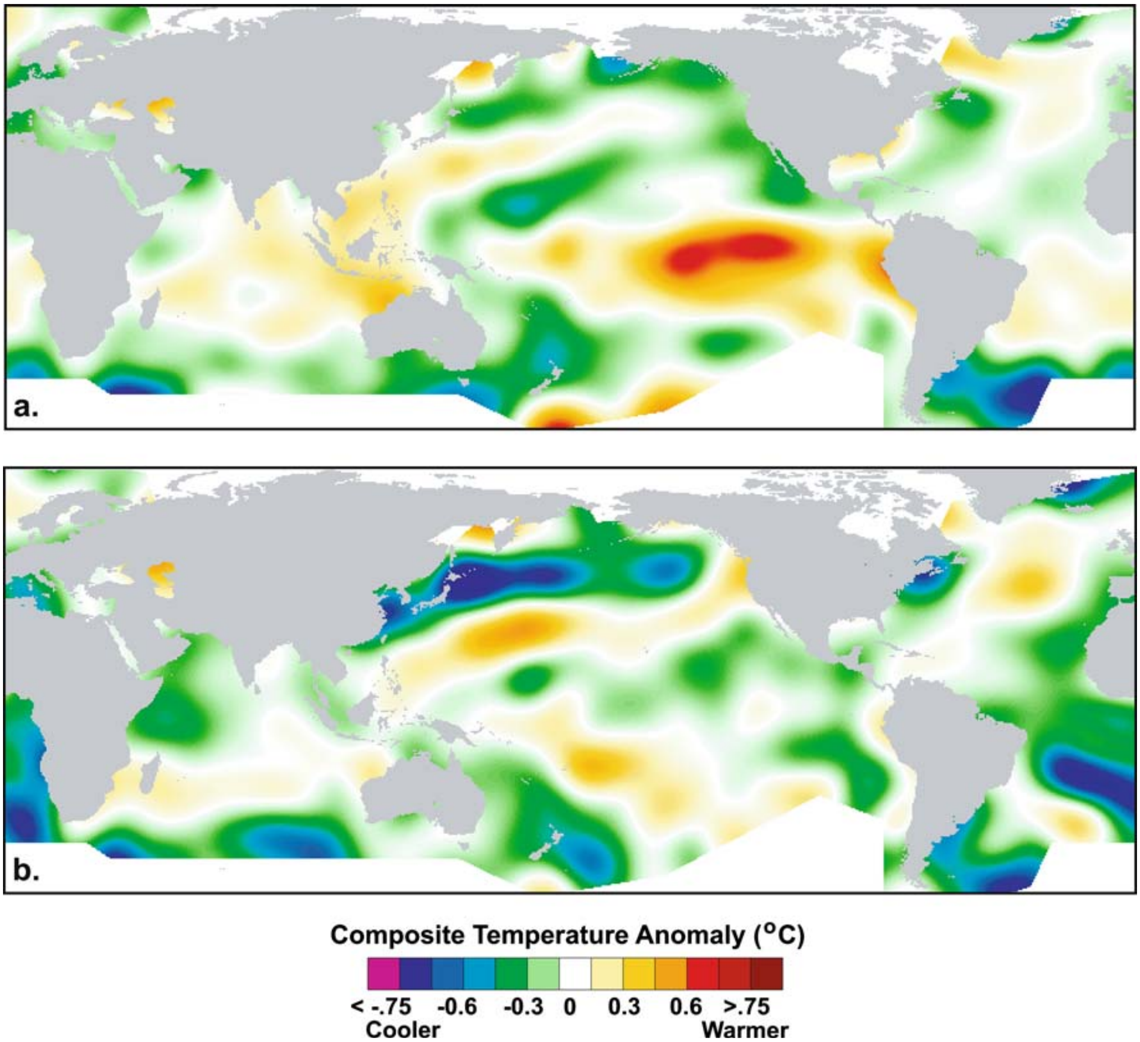

Fig. 7 Composite maps of global SST anomalies during the ten driest (**a**) and ten wettest (**b**) years in the rainfall reconstruction since 1857 show the importance of SSTs in the eastern Pacific and possibly the Atlantic and Indian Oceans. This supports a link between ENSO variability and the ~3.4 year spectral peak observed in the reconstruction (Fig. 6)

of November–February precipitation variability over the past two centuries though low sample size prior to 1870 suggest cautious interpretation in this period. The reconstruction identifies drought for seven consecutive years in the 1880s when the chronology is fairly well replicated, and this event is matched only by one 8-year event in the instrumental record. The reconstruction also suggests that a drought as much as 10-years long in the 1860s may have exceeded similar events in the modern observational record. Multi-decadal trends in rainfall such as that observed since about 1960 also appear to have occurred in the past. The reconstruction should be useful in conjunction with other proxy climate data from the region such as historical records to study the spatial and temporal extent of extreme climate prior to the observational period.

Spectral analysis of the reconstruction indicates a significant peak at ~3.4 years, which may be related to the influence of the ENSO. Composite analysis of SSTs during the driest years in Zimbabwe indicates an association with warm SSTs in the eastern equatorial Pacific. The reconstruction is also significantly correlated with maize yield in Zimbabwe and this relationship could provide useful information regarding the impact of past climate on agriculture.

These results indicate that *P. angolensis* will be a valuable species for the reconstruction of climate in southern Africa. Standard 5 mm diameter core samples extracted with a Swedish increment borer are unfortunately not adequate for exact dendrochronological crossdating because of the complex poorly-defined anatomy of the annual growth rings in this species. Cross sections with at least 10 cm surface area are adequate and have been obtained from stumps and logs following timber extraction. Mukwa is currently being heavily exploited in many areas of southern Africa so tree-ring specimens can be salvaged for the development of a widespread network of climate-sensitive tree-ring chronologies in the region. Development of this network will provide important new information about past climate as well as data on growth rates and other ecological attributes, which should be valuable for the sustainable management of this commercially important lumber species. The new chronology and reconstruction data are available from the National Geophysical Data Center Website (http://www.ngdc.noaa.gov/paleo)

Acknowledgements This research was supported by The University of Virginia Center for Regional Environmental Studies and NASA Award NNG-04-GM71G, and the US National Science Foundation Earth System History Program (ATM-0400713). We thank C. Bullen, E. February, F. Fye, G. Haynes, M. Mukelabai, P. Mushove (deceased) D. Ngwako, The Botswana Department of Agriculture, Rangeland Ecology Division, The Zambian Meteorological Department, The Zimbabwe Forest Industries Training Center, Mutare, The Zimbabwe Forestry Commision, The Zimbabwe Forest Research Center, Harare.

References

Allan H, Lindsay J, Parker D (1996) Ela Niño/Southern Oscillation & Climate Variability. CSIRO Publishing, pp 408

von Breitenbach F (1973) Pterocarpus Angolensis: A Monograph. Trees in South Africa 25:58–80

Briffa K (1995) Interpreting high-resolution proxy climate data—the example of dendroclimatology. In: von Storch H, Navarra A (eds) Analysis of climate variability, applications of statistical techniques. Springer, Berlin Heidelberg NewYork, pp 77–94

Cane MA, Eshel G, Buckland RW (1994) Forecasting Zimbabwean maize yield using eastern equatorial Pacific sea surface temperature. Nature 370:204–205

Coates Palgrave K (1983) Trees of Southern Africa. 2nd edn. Struik, Cape Town, pp 959

Cook ER (1985) A times series analysis approach to tree-ring standardization. PhD thesis, University of Arizona

Cook E, Kairiukstis L (1990) Methods of dendrochronology: applications in the environmental sciences. Kluwer, Dordrecht

Douglass AE (1941) Crossdating in dendrochronology. J Forest 39(10):825–831

Draper N, Smith H (1981) Applied regression analysis. 2nd edn. Wiley, New York, pp 709

Dunwiddie PW, LaMarche Jr. VC (1980) A climatically responsive tree-ring record from Widdringtonia cedarbergensis, Cape Province, South Africa. Nature 286:796–797

Durbin J, Watson GS (1950) Testing for serial correlation in least squares regression I. Biometrika 37:409–428

FAO (2004) Food and agricultural organization of the United Nations. http://www.faostat.fao.org/faostat/

February EC, Gagen M (2003) A dendrochronological assessment of two South African Widdringtonia species. S Afr J Bot 69(3):428–433

February EC, Stock WD (1998) An assessment of the dendrochronological potential of two Podocarpus species. Holocene 8(6):747–750

Fichtler E, Trouet V, Beeckman H, Coppin P, Worbes M (2004) Climatic signals in tree rings of Burkea africana and Pterocarpus angolensis from semiarid forests in Namibia. Trees 18:442–451

Fritts HC (1976) Tree rings and climate. Blackburn Press, Clarendan, pp 567

Fritts HC (1990) Modeling tree-ring and environmental relationships for dendrochronological analysis. In: Dixon RK, Meldahl RS, Ruark GA, Warren WG (eds) Process modeling of forest growth responses to environmental stress. Timber Press, Portland pp 368–382

Holmes RL (1983) Computer-assisted quality control in tree-ring dating and measurement. Tree Ring Bull 43:69–78

Holmgren K (2002) Climate reconstructions from speleothems in southern Africa ESF–HOLIVAR workshop, Lammi Finland, April 17–20th 2002

Hulme M (1992) A 1951–80 global land precipitation climatology for the evaluation of general circulation models. Clim Dyn 7:57–72

Hulme M (1994) Validation of large-scale precipitation fields in general circulation models. In: Desbois M, Desalmand F (eds) Global precipitation and climate change NATO ASI series. Springer, Berlin Heidelberg New York, pp 387–406

Hulme M, Osborn TJ, Johns TC (1998) Precipitation sensitivity to global warming: comparison of observations with HadCM2 simulations. Geophys Res Lett 25:3379–3382

Jenkins GM, Watts DG (1968) Spectral analysis and its applications, Holden Day, San Francisco, pp 525

Jury MR (1996) Regional teleconnection patterns associated with summer rainfall over South Africa, Namibia and Zimbabwe. Int J Climatology 16:135–153

Kaplan A, Cane M, Kushnir Y, Clement A, Blumenthal M, Rajagopalan B (1998) Analysis of global sea surface temperature 1856–1991. J Geophys Res 103:18567–18589

Krishna Kumar, Rajagopalan B, Cane MA (1999) On the weakening relationship between the Indian monsoon and ENSO. Science 284:2156–2159

Lindesay JA, Vogel CH (1990) Historical evidence for southern oscillation–southern African rainfall relationships. Int J Climatology 10:679–689

Makarau A, Jury MR (1996) Predictability of Zimbabwe summer rainfall. Int J Climatology 17:1421–1432

Mason SJ (2001) El Niño climate change, and southern African climate. Envr Mtrc 12:327–345

Mason SJ, Jury MR (1997) Climatic change and variability over southern Africa: a reflection on underlying processes. Prog Phys Geogr 21:23–50

Moron V, Ward MN (1998) ENSO teleconnections with climate variability in the European and African sectors. Weather 9:287–295

Nash DJ, Endfield GH (2002) A 19th century climate chronology for the Kalahari region of central southern Africa derived from missionary correspondence. Int J Climatology 22:821–841

Nicholson SE (1979) The methodology of historical climate reconstruction and its application to Africa. J Afr Hist 20:31–49

Nicholson SE (1981) The historical climatology of Africa. In: Wigley TML, Ingram MJ, Farmer G (eds) Climate and history. Cambridge Press, Cambridge, pp 249–270

Nicholson SE (1994) Recent rainfall fluctuations in Africa and their relationships to past conditions over the continent. Holocene 4:121–131

Nicholson SE, Entekhabi D (1986) The quasi-periodic behavior of rainfall variability in Africa and its relationship to the southern oscillation. J Clim Appl Met 34:331–348

Nicholson SE, Entekhabi D (1987) Rainfall variability in equatorial and southern Africa. Relationships with sea-surface temperatures along the southwestern coast of Africa. J Clim Appl Met 26:561–578

Nicholson SE, Kim J (1997) The relationship of the El Niño-southern oscillation to African rainfall. Int J Climatology 17:117–135

Phillips JG, Cane MA, Rosenzweig C (1998) ENSO, seasonal rainfall patterns and simulated maize yield variability in Zimbabwe. Agri Forest Met 90:39–50

Ropelewski CF, Halpert MS (1987) Global and regional scale precipitation and temperature patterns associated with El Niño/Southern Oscillation. Mon Weath Rev 115:1606–1626

Ropelewski CF, Halpert MS (1989) Precipitation patterns associated with the high index phase of the southern oscillation. J Climate 2:268–284

Schulman E (1956) Dendroclimatic changes in semiarid America. Arizona Press, Tucson, 142 pp

Shackleton CM (2002) Growth patterns of Pterocarpus angolensis in savannas of the South African lowveld. For Ecol Man 166:85–97

Stahle DW (1999) Effective strategies for the development of tropical tree-ring chronologies. IAWA J 20:249–253

Stahle DW, Mushove PT, Cleaveland MK, Roig F, Haynes GA (1999) Management implications of annual growth rings in Pterocarpus angolensis from Zimbabwe. For Ecol Man 124:217–229

Stokes MA, Smiley TL (1996) An introduction to tree ring dating. Arizona Przess, Tucson

Thackeray JF (1996) Ring width variation in a specimen of South African Podocarpus, circa 1350–1937 AD. Palaeoecol Afr 24:233–240

Torrence C, Webster PJ (1999) Interdecadal changes in the ENSO–monsoon system. J Clim 12:2679–2690

Trouet V (2004) The El Niño Southern Oscillation effect on Zambezian miombo vegetation:proxies from tree ring series and satellite-derived data. PhD thesis, Catholic University

Trouet V, Haneca K, Coppin P, Beeckman H (2001) Tree ring analysis of Brachystegia spiciformis and Isoberlina tomentosa: evaluation of the ENSO-signal in the miombo woodland of Eastern Africa. IAWA J 22:385–399

Tyson PD (1986) Temporal and spatial variations of rainfall anomalies in Africa south of latitude 22° during the period of meteorological record. Clim Change 2:363–371

Tyson PD, Cooper GRJ, McCarthy TS (2002) Millennial to multi-decadal variability in the climate of southern Africa. Int J Climatology 22:1105–1117

Verschuren D, Laird KR, Cumming BF (2000) Rainfall and drought in equatorial East Africa during the past 1100 years. Nature 403:410–414

Vogel C (1989) A documentary-derived climatic chronology for South Africa. Clim Change 14:291–308